



**Yang, Wenbin and Lunn, Rebecca J and Tarantino, Alessandro and El Mountassir, Grainne (2017) Laboratory testing of a MEMS sensor system for in-situ monitoring of the engineered barrier in a geological disposal facility. *Geosciences*, 7 (38). ISSN 2076-3263 , <http://dx.doi.org/10.3390/geosciences7020038>**

This version is available at <https://strathprints.strath.ac.uk/60654/>

**Strathprints** is designed to allow users to access the research output of the University of Strathclyde. Unless otherwise explicitly stated on the manuscript, Copyright © and Moral Rights for the papers on this site are retained by the individual authors and/or other copyright owners. Please check the manuscript for details of any other licences that may have been applied. You may not engage in further distribution of the material for any profitmaking activities or any commercial gain. You may freely distribute both the url (<https://strathprints.strath.ac.uk/>) and the content of this paper for research or private study, educational, or not-for-profit purposes without prior permission or charge.

Any correspondence concerning this service should be sent to the Strathprints administrator: [strathprints@strath.ac.uk](mailto:strathprints@strath.ac.uk)

1 Article

# 2 Laboratory Testing of a MEMS Sensor System for In-situ 3 Monitoring of the Engineered Barrier in a Geological Disposal 4 Facility

5 Wenbin Yang<sup>1</sup>, Rebecca J Lunn<sup>1,\*</sup>, Alessandro Tarantino<sup>1</sup> and Gráinne El Mountassir<sup>1</sup>

6 <sup>1</sup> Department of Civil and Environmental Engineering, University of Strathclyde, Glasgow G1 1XJ

7 \* Correspondence: Rebecca.lunn@strath.ac.uk; Tel.: +44-141-548-2826

8 Academic Editor: Xiaozhen Han

9 Received: date; Accepted: date; Published: date

10 **Abstract:** Geological disposal facilities for radioactive waste pose significant challenges for robust  
11 monitoring of environmental conditions within the engineered barriers that surround the waste  
12 canister. Temperatures are elevated, due to the presence of heat generating waste, relative  
13 humidity varies from 20% to 100%, and swelling pressures within the bentonite barrier can  
14 typically be 2-10 MPa. Here, we test the robustness of a bespoke design MEMS sensor-based  
15 monitoring system, which we encapsulate in polyurethane resin. We place the sensor within an  
16 oedometer cell and show that despite a rise in swelling pressure to 2 MPa, our relative humidity  
17 (RH) measurements are unaffected. We then test the sensing system against a traditional RH  
18 sensor, using saturated bentonite with a range of RH values between 50% and 100%.  
19 Measurements differ, on average, by 2.87% RH, and are particularly far apart for values of RH  
20 greater than 98%. However, bespoke calibration of the MEMS sensing system using saturated  
21 solutions of known RH, reduces the measurement difference to an average of 1.97% RH, greatly  
22 increasing the accuracy for RH values close to 100%.

23 **Keywords:** monitoring; geological disposal; sensor; relative humidity; bentonite; engineered  
24 barrier system; MEMS; geological disposal

---

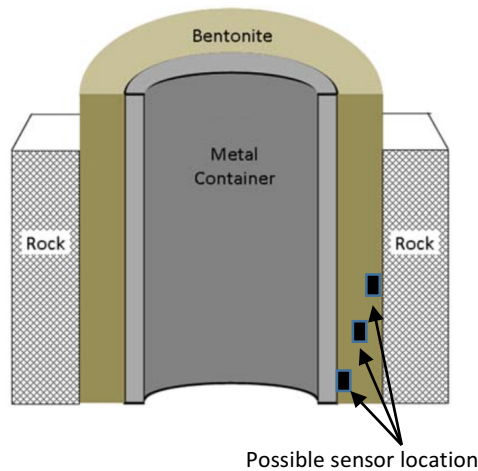
## 26 1. Introduction

27 Real-time monitoring of deep geological disposal facilities (GDFs) for radioactive waste  
28 disposal is a significant challenge. The operational timescales of a GDF mean that monitoring  
29 technologies must function reliably over timescales in excess of 100 years [1]. A regulatory  
30 requirement of any GDF is likely to be the *in-situ* monitoring of the  
31 thermo-hydro-mechanical-chemical (THMC) behaviour of the engineered barrier system (EBS) that  
32 surrounds the waste canister. Monitoring creates significant challenges, temperatures can be highly  
33 elevated due to the presence of heat generating waste, relative humidity (RH) varies from 20% to  
34 100%, and swelling pressures within the bentonite barrier are typically in excess of 2 MPa.

35 Most geological disposal concepts, for example the Swedish KBS-3V concept, are based on an  
36 EBS composed of a compacted bentonite buffer, which surrounds the waste canister (e.g. Figure 1).  
37 Post deposition, the bentonite buffer saturates via groundwater ingress from the surrounding rock,  
38 which results in a swelling pressure of between 2 and 10 MPa to ensure hydraulic sealing between  
39 the EBS, the surrounding rock and the central waste canister. Further, the very low hydraulic  
40 permeability of the bentonite ensures that, should canister failure occur, radionuclide transport  
41 would be extremely slow, since it is via diffusion only. Finally, the plastic nature of the saturated  
42 bentonite within the EBS also protects the canister from structural damage during small earthquakes  
43 [2].

44 Historically, an extensive range of relative humidity sensors have been deployed in radioactive  
45 waste disposal facilities and in underground testing laboratories over the past decades [3, 4]. While

46 the measurement principle of the sensors varies, one common restraint of these traditional sensors  
 47 lies in the unit size of the sensor (typically in the order of 10 cm), which limits the spatial resolution  
 48 of the sensing device.  
 49



50  
 51 **Figure 1.** Schematic cross-section through the bentonite engineered barrier system  
 52

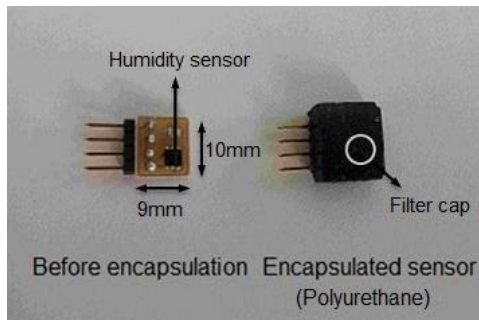
53 This research focuses on testing of a MEMS-based (Micro-Electro-Mechanical System) sensing  
 54 system, developed in [5] for monitoring relative humidity within, or adjacent to, the compacted  
 55 bentonite buffer in the EBS. Application of MEMS sensors in GDFs and other civil engineering  
 56 projects still faces several key challenges in the engineering field [6]. This paper extends our  
 57 previous research [5] by testing the performance of bespoke encapsulated MEMS sensors within  
 58 saturated bentonite under swelling pressures of 2MPa. We show that our encapsulated MEMS  
 59 monitoring system can withstand swelling pressures in excess of 2MPa and that, through improved  
 60 sensor calibration, accurate measurements of compacted bentonite relative humidity can be  
 61 achieved even up to RH values of 100%.

## 62 2. Materials and Methods

63 MEMS sensors provide higher measurement accuracy, improved spatial resolution in a limited  
 64 space, and a longer life cycle resulting from low power consumption in the order of microwatts [7].  
 65 A first prototype of a multi-sensor monitoring system was presented in [5]. The system contains the  
 66 Maxim® 31725 temperature sensor [8] and the Sensirion® SHT25 relative humidity sensor [9]. The  
 67 Maxim® 31725 temperature sensor has a typical precision of  $\pm 0.5^\circ\text{C}$  for a measurement range  
 68 between  $-55^\circ\text{C}$  and  $150^\circ\text{C}$ , and the Sensirion® SHT25 RH sensor has a labelled precision level of  
 69  $\pm 1.8\%$  within the 10%-90% RH range, and  $\pm 3\%$  for the full RH range. Both sensors have a chip  
 70 dimension of 3mm x 3mm x 1mm, and are integrated onto a single printed circuit board (Figure 2).  
 71 To minimise size, the sensor block 9mm x 11mm, is limited to hosting the sensor and its connector,  
 72 all other functional components are integrated onto the motherboard that can be installed outside  
 73 the bentonite barrier. The power supply and signal transmission are maintained by heat-resistant  
 74 PTFE-coated wires that are compatible with temperatures between  $-60^\circ\text{C}$  and  $200^\circ\text{C}$ . In future, these  
 75 wires are planned for replacement by a wireless transmission system, which eliminates wire  
 76 installation concerns, although at the expense of slightly increased sensor size.

77 To avoid direct contact between the sensor and the bentonite, a PTFE filter membrane cap  
 78 designed by Sensirion® [10] was incorporated to cover the RH sensor on the PCB board prior to  
 79 encapsulation. The filter protects the sensor from mechanical impact and contamination and  
 80 prevents liquid water entering the sensors by capillarity, thus invalidating the measurement. At the  
 81 same time, it allows the propagation of water vapour molecules between the measuring  
 82 environment and the RH sensor. The sensor was then encapsulated via a 'potting' method [11] that  
 83 uses polyurethane resin as an encapsulation material. This resulted in a rectangular polyurethane

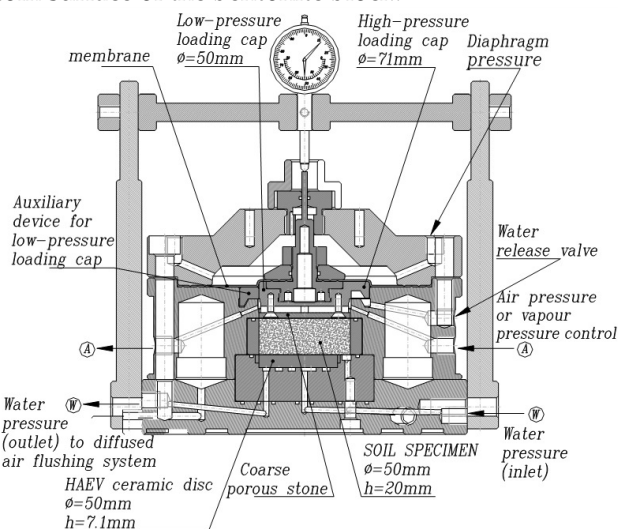
84 block that enclosed the sensor, with window for the measurement of RH (Figure 2). The  
 85 encapsulated sensor block has similar dimensions to the sensor board prior to encapsulation, thus  
 86 maintaining the small size. Since the MEMS temperature sensor is entirely encompassed during  
 87 polyurethane encapsulation, it is unaffected by the bentonite, so is not discussed further. By contrast,  
 88 the RH humidity sensor relies on detection through the sensing window (Figure 2) and its accuracy  
 89 may be compromised either by contact via liquid phase with the pore-water of the saturated  
 90 bentonite, or by the swelling pressure that is exerted.  
 91



92  
 93 **Figure 1** SHT25 sensor board before and after encapsulation  
 94

95 Experiment 1 focuses on verifying the mechanical robustness of the RH sensor under the  
 96 swelling pressure exerted by hydrated bentonite. The test was carried out in an engineered  
 97 oedometer cell, specifically designed by the Universitat Politècnica de Catalunya, as shown in Figure  
 98 3. The oedometer cell is separated into two sections by a ceramic-disc-supported thin membrane. On  
 99 top of the membrane an enclosed water reservoir is used to apply a known vertical stress to the top  
 100 of the sample within the range 0 – 2 MPa. A compacted bentonite block was fitted in the cavity below  
 101 the membrane. The compacted MX-80 bentonite was drilled to form a 20mm-thick cylinder block,  
 102 with a diameter of 50mm. The size of the bentonite block corresponded exactly to the dimension of  
 103 the cavity inside the oedometer cell, in order to ensure that the top surface of the bentonite block was  
 104 in firm contact with the membrane.

105 Hydration of the bentonite occurred through injection of deionised water from channel A  
 106 (Figure 3) onto the top surface of the bentonite. The gap between the bentonite block and the side  
 107 ring of the oedometer was sealed by polyurethane resin, in order to inhibit the ingress of water  
 108 down the sides of the bentonite so as to achieve uni-directional water flow from the top surface to  
 109 the bottom surface of the bentonite block.

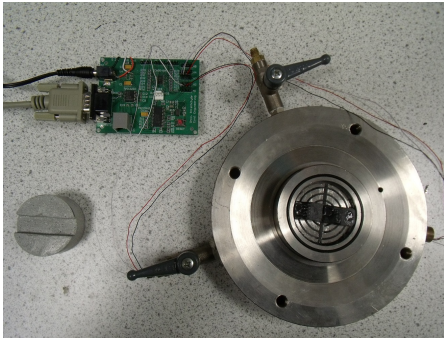


110  
 111 **Figure 2** Cross-sectional structure of the oedometer cell  
 112

113 In order to insert two sensors (side-by-side), a rectangular groove was carved into the base of  
 114 the bentonite block, as shown in Figure 4. Two RH sensors were fitted into the groove, ensuring a

115 firm contact with the bentonite block. This allowed the relative humidity at the bottom of the  
 116 bentonite block to be measured during hydration. This installation minimised the volume of air  
 117 between the sample and the sensor ensuring a rapid response time. The electrical wires connecting  
 118 the sensors to the control system were meticulously guided through channels beneath the cavity to  
 119 the outside of the oedometer cell, and connected to the controller board. The exterior entrances to  
 120 these channels were sealed via application of polyurethane, in order to block the air ventilation  
 121 through the channel, and hence to prevent pore-water evaporation from the sample and, most of all,  
 122 water vapour flow through any gap between the sample and the sensor towards the outside of the  
 123 cell.

124



125

126

**Figure 3** Placement of the RH sensors in the oedometer and the groove at the bottom of the bentonite

127

128

129

130

131

132

133

134

135

136

137

138

139

140

141

142

143

144

145

146

$$\Psi = -\frac{RT}{v_{w0}\omega_v} \ln\left(\frac{u_v}{u_{v0}}\right) = -\frac{RT}{v_{w0}\omega_v} \ln(RH), \quad (\text{Equation 1})$$

147

148

149

150

151

152

153

$$\Psi = -135022 \ln(RH), \quad (\text{Equation 2})$$

154

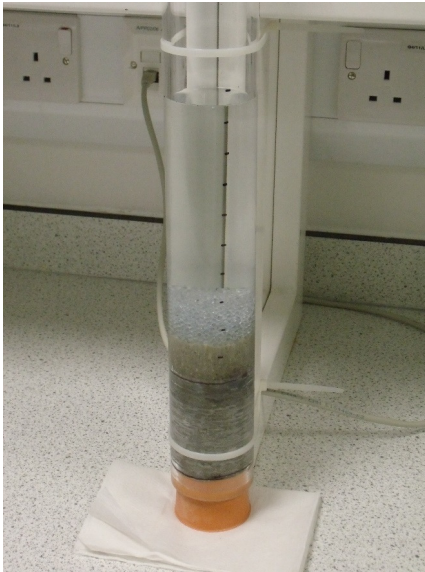
155

156

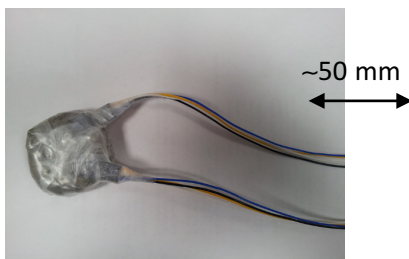
157

where  $\Psi$  is given in kPa. This equation was used to derive the relative humidity RH measured in the air surrounding the sample from the value of total suction  $\Psi$  displayed by the instrument.

158 By comparing the RH measured using a WP4 dewpoint potentiometer with the RH measured  
 159 by the sensing system, within the same hydrated bentonite block, we can validate the *in-vivo*  
 160 measurement accuracy of the RH sensor whilst embedded in a bentonite block.  
 161



162  
 163 **Figure 4** Hydration of bentonite block in polycarbonate tube  
 164



165  
 166 **Figure 5** Hydrated bentonite block wrapped with RH sensors  
 167

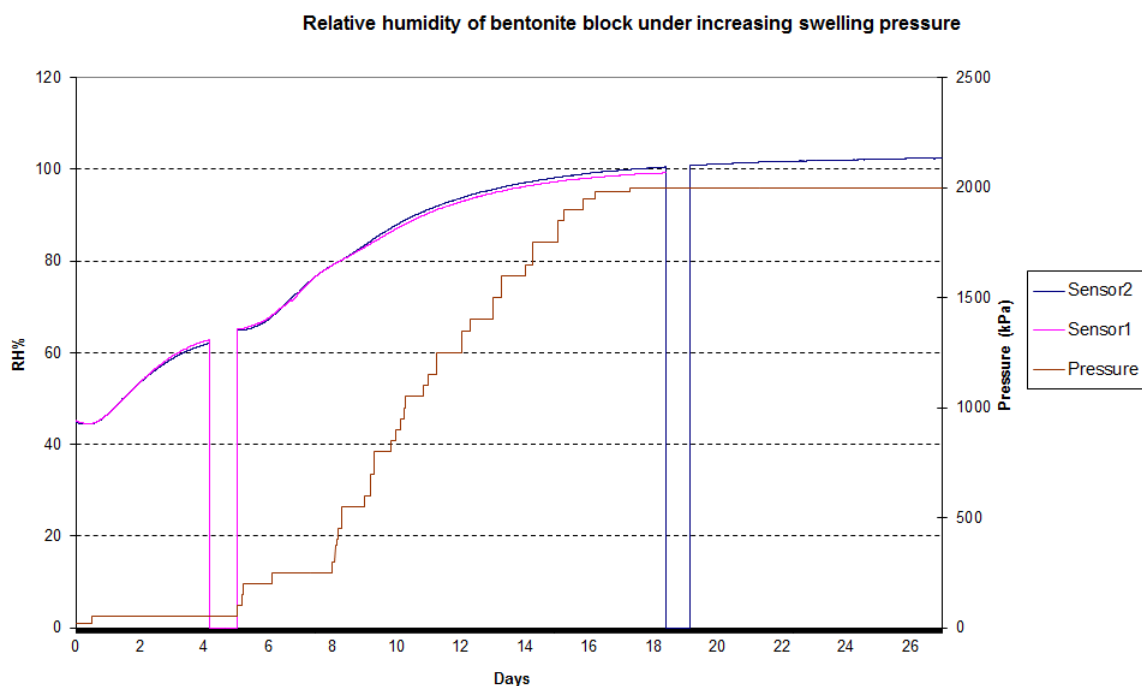
168 Experiment 2 was carried out using the following steps: an MX-80 bentonite block was first cut  
 169 and drilled to form a short cylinder with a diameter of 5cm and a height of approximately 7.5cm. The  
 170 bentonite cylinder was then sealed on the sides using an impermeable membrane and fixed to the  
 171 bottom of a polycarbonate tube, as shown in Figure 5. The internal diameter of the tube was chosen  
 172 to be the same as the diameter of the bentonite cylinder, with any remaining void space between the  
 173 bentonite and the tube wall being filled by the membrane. Water was injected from the top of the  
 174 tube and was only in contact with the upper surface of the bentonite block. Hence, the hydration of  
 175 the bentonite block took place gradually from top to bottom, and a gradient of water content along  
 176 the length of the bentonite cylinder was formed during this hydration process.

177 The duration of the hydration process varied between tests with a minimum of 7 days and a  
 178 maximum of 20 days. This was to achieve different water content levels in the bentonite samples  
 179 such that sensor accuracy could be tested at a range of relative humidity values. The hydrated  
 180 bentonite block was then removed from the tube and cut into slices approximately 2.5cm thick.  
 181 Rectangular cavities were cut into both sides of each 2.5 cm bentonite block to install the RH sensors.  
 182 The hydrated bentonite block and the sensors were then wrapped using an impermeable membrane  
 183 to allow for water vapour equilibrium in the air surrounding the sample, as shown in Figure 6. The  
 184 RH data was regularly measured by the sensing system over a period of several days until a constant  
 185 RH was recorded, indicating that i) uniform distribution of suction was achieved within the  
 186 bentonite block and ii) water vapour surrounding the bentonite block achieved equilibrium with  
 187 suction in the bentonite. The bentonite block was then unsealed and a small sample of each block  
 188 was immediately put into the WP4. The RH of the sample could be calculated from the displayed  
 189 value of total suction  $\Psi$  using equation 5.2.

190

191 **3. Results**192 *3.1. Mechanical Robustness of the Sensing System*

193 The results of Experiment 1, the oedometer cell test, are plotted in Figure 7. Shown is the relative  
 194 humidity measured by both RH sensors alongside the increase in total vertical stress (water pressure  
 195 controlled by the GDS), in turn associated with the swelling pressure generated by the progressive  
 196 hydration of the sample. A temporary signal loss occurred between days 4 and 5 and days 18 and 19,  
 197 caused by a bad contact on the sensor-to-wire connector under the influence of the increasing  
 198 swelling pressure. The connection for sensor 1 did not recover. Both sensors, however, are fully  
 199 functional during the entire experimental period of 26 days and remain unaffected by a swelling  
 200 pressure of >2MPa, which was maintained for a 10-day period. It is worth noting that the swelling  
 201 pressure and the RH recorded by the two sensors level off at the same time, highlighting the  
 202 coherence of the RH measurement.



203

204 **Figure 7** Evolution of relative humidity and GDS water pressure during the hydration of the bentonite within  
 205 the oedometer cell

206 At the end of the experiment, both sensors were removed from the oedometer cell and tested again  
 207 in the open air. Test results revealed that both sensors were fully functional after sustaining the high  
 208 swelling pressure, without any deterioration in sensor accuracy. The swelling pressures tested here  
 209 are at the lower end of those that would be experienced in a geological disposal facility, sensor  
 210 performance was entirely unaffected and the sensors proved to be robust. The observed signal loss  
 211 would be eliminated by more robust cable connection methods (these were soldered by hand) or by  
 212 the incorporation of a wireless transmission onto the sensing system.

213 *3.2. Sensor accuracy within the saturated bentonite*

214 Table 1 shows the results for both measurement methods (WP4 and RH sensing system) for seven  
 215 different bentonite samples, as described for Experiment 2, covering a range of RH levels from 52%  
 216 to 100%. Analysis of the data in Table 1 shows that the RH measured by the two methods is

217 generally coherent, but with a mean discrepancy of 2.87(%RH). With the exception of sample No. 1,  
 218 sample differences are less than 4%. For sample No. 1, at very high humidity there is a discrepancy  
 219 of 8.1%.

220 **Table 1** RH for seven hydrated bentonite samples from Experiment 2, measured by psychrometer and by the  
 221 sensor

Sample No.	Suction (MPa)	RH calculated from suction	RH measured by sensor	Difference
1	-0.09 MPa	99.9%	108.0%	-8.10%
2	-5.22 MPa	96.2%	97.8%	-1.60%
3	-9.47 MPa	93.3%	97.1%	-3.80%
4	-34.76 MPa	77.4%	76.8%	0.60%
5	-44.69 MPa	71.9%	73.1%	-1.20%
6	-83.55 MPa	54.1%	52.0%	2.10%
7	-96.94 MPa	49.0%	51.7%	-2.70%

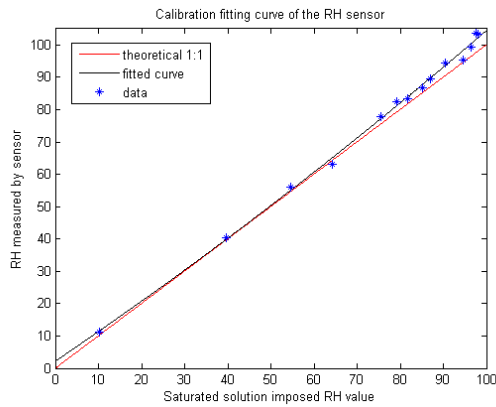
222

#### 223 4. Discussion

224 The differences noted between the measurements of the sensing system developed here may be due  
 225 both to errors in the WP4 measurement and/or the sensor measurement. The WP4 method tends to  
 226 underestimate relative humidity due to invasion of ambient air into the sealed sample chamber,  
 227 allowing some evaporation until equilibrium is established [12]. The WP4 also tends to be inaccurate  
 228 at RH values close to 100%, when even very small fluctuations of temperature can cause drop  
 229 condensation in the measurement chamber. Table 1 suggests the latter error has not been an issue:  
 230 among the different measurement techniques, the WP4 is perhaps the one that ensures the largest  
 231 measurement range at high RH values (up to 99.0-99.5%). Other commercial RH sensors, including  
 232 thermocouple and transistor psychrometers, are characterised by a shorter measurement range (up  
 233 to 98.5-99.0%) [13].

234 For the case of the RH MEMS sensor tested in this experimental programme, another source of  
 235 inaccuracy is the non-linearity of the relationship between the air relative humidity and the  
 236 volumetric water content of the hygroscopic dielectric material placed between the two plates of the  
 237 capacitive sensor. When relative humidity approaches 100%, the sensing element approaches  
 238 saturation. As a result, variations in RH generate variations in volumetric water content of the  
 239 dielectric material that tend to become smaller and smaller as saturation is approached. In turn,  
 240 variations in capacitance and, hence, electrical signal, tend to become negligible. Since the derivative  
 241 of the capacitance versus RH function tends to zero as saturation is approached, there is a loss of  
 242 sensitivity of the instrument close to saturation.





243

244 **Figure 8** Fitting curve of the calibration model for the RH sensor

245 This loss in accuracy associated with the non-linearity of the calibration curve was quantified in [5]  
 246 by the use of a variety of saturated chemical solutions, each of which had a different, known  
 247 saturated relative humidity when placed within a sealed, temperature-controlled environment.  
 248 Hence, these could be used as accurate reference points without the requirement for any type of  
 249 sensor. The results of these experiments are reproduced in Figure 10. Data points lie on the 1:1 line  
 250 (in red) in the low to medium RH range, but deviate consistently at high RH values. If the relative  
 251 humidity values returned by the sensor RH are treated as raw sensor data, the sensor can be  
 252 calibrated using the fitted curve in Figure 10. An adjusted estimate of the relative humidity  $RH_A$  can  
 253 be from the calibration equation in Figure 10 is:

254  $RH=0.001204(RH_A)^2+0.9015RH_A+2.182$ , (Equation 3)

255 Solving this quadratic equation gives an adjusted value of the measured relative humidity based on  
 256 the sensor calibration curve,  $RH_A$ . The adjusted values for relative humidity  $RH_A$  are shown in Table  
 257 2. The difference between the measured value ( $RH_A$ ) and that derived from the WP4 data has now  
 258 reduced. The mean of the differences between them is now 1.97% and the discrepancy between the  
 259 two values for sample number 1, at high humidity, has dropped from 8.1% to 1.9%.

260 MEMS sensor systems are considerably smaller than traditional monitoring devices, allowing  
 261 accurate point measurements (as opposed to spatially averaged) and far less physical disturbance to  
 262 the engineered barrier system within a repository. The results of both Experiment 1 and Experiment  
 263 2 described here, show that our MEMS-based sensing system is a promising miniaturised alternative  
 264 to traditional RH sensors in geological disposal facilities. It is sufficiently robust to withstand at least  
 265 2MPa of swelling pressure and, once calibrated, is capable of accurate RH measurement over the  
 266 wide range of RH values (20% - 100%) encountered within an EBS.

267 **Table 2** Corrected RH of hydrated bentonite samples measured by psychrometer and by the sensor

Sample No.	RH calculated from suction	$RH_A$ corrected	Difference
1	99.9%	101.8%	-1.90%
2	96.2%	93.1%	3.10%
3	93.3%	92.6%	0.70%
4	77.4%	74.7%	2.70%
5	71.9%	71.3%	0.60%
6	54.1%	51.6%	2.50%
7	49.0%	51.3%	-2.30%

268

269

270 **Acknowledgments:** This research has been supported by EPSRC consortium grant EP/I036427/1 ‘SAFE Barriers  
271 – a Systems Approach For Engineered Barriers’ (2012-2016). This was co-funded by EPSRC and Nuclear  
272 Decommissioning Authority Radioactive Waste Management Directive, now Radioactive Waste Management”.

273

274 **References**

275

276 1. Lidskog, R. and Andersson, A.C. (2002) The Management of Radioactive Waste: A Description of Ten  
277 Countries. SKB report, ISBN 91-973987-3-X.

278 2. Juvankoski, M., Ikonen, K., and Jalonen, T. (2012) Buffer production line 2012: Design, production and  
279 initial state of the buffer. Posiva report 2012-17.

280 3. Alonso, E.E., Springman, S.M. and Ng, W.W. (2009) Monitoring large-scale tests for nuclear waste  
281 disposal. *Geotechnical and Geological Engineering*, 26, 817–826.

282 4. Breen, B.J., Garcia-Sineriz, J.L., Maurer, H., Mayer, S., Schröder, T.J. and Verstricht, J. (2012) EC MoDeRn  
283 Project: In-situ demonstration of innovative monitoring technologies for geological disposal. WM2012  
284 Conference. Available at [www.wmsym.org/archives/2012/papers/12053.pdf](http://www.wmsym.org/archives/2012/papers/12053.pdf)

285 5. Yang W., Lunn R.J. and Tarantino A. (2015) MEMS sensor-based monitoring system for engineered  
286 geological disposal facilities. *Mineralogical Magazine*. Vol. 79(6): 1475–1483.

287 6. Ceylan H., Gopalakrishnan, K., Taylor, P., Shrotriya, P., Kim, S., Prokudin, M., Wang, S., Buss, A.F.,  
288 Zhang, J. et al. (2011) A Feasibility Study on Embedded Micro-electromechanical Sensors and Systems  
289 (MEMS) for Monitoring Highway Structures. Iowa Highway Research Board Report No. TR-575.

290 7. Akyildiz, I.F., Su, W., Sankarasubramaniam, Y. and Cayirci, E. (2002) Wireless sensor networks: a survey.  
291 *Computer Networks*, 38, 393–422.

292 8. Maxim® 31725 datasheet. Ver.2013. Available from:  
293 <http://datasheets.maximintegrated.com/en/ds/MAX31725-MAX31726.pdf>

294 9. Sensirion® SHT25 datasheet. Ver.2014. Available from:  
295 [http://www.sensirion.com/fileadmin/user\\_upload/customers/sensirion/Dokumente/Humidity/Sensirion\\_Humidity\\_SHT25\\_Datasheet\\_V3.pdf](http://www.sensirion.com/fileadmin/user_upload/customers/sensirion/Dokumente/Humidity/Sensirion_Humidity_SHT25_Datasheet_V3.pdf)

296 10. Sensirion® Filter Cap SF2 datasheet. Ver.2011. Available from: <http://www.sensirion.com/sf2/>

297 11. Chao, N. H., Dispenza, J. A. and DeAngelis, M. E. (2012) Encapsulating protective layers for enhancing  
298 survivability of circuit board assemblies in harsh and extreme environments, *ASME 2012 International  
299 Mechanical Engineering Congress and Exposition*, 9, 363-373

300 12. Cardoso R., Romero E., Lima A., Ferrari A. (2007) A Comparative Study of Soil Suction Measurement  
301 Using Two Different High-Range Psychrometers. In: Schanz T. (eds) *Experimental Unsaturated Soil  
302 Mechanics*. Springer Proceedings in Physics, vol 112. Springer, Berlin, Heidelberg.

303 13. Bulut, R., Leong, E.C. (2008). Indirect measurement of suction. *Geotechnical and Geological Engineering*,  
304 26(6): 21-32.  
305



© 2017 by the authors. Submitted for possible open access publication under the terms and conditions of the Creative Commons Attribution (CC BY) license (<http://creativecommons.org/licenses/by/4.0/>).